XII International Conference on Computational Plasticity. Fundamentals and Applications
COMPLAS XII
E. Oñate, D.R.J. Owen, D. Peric and B. Suárez (Eds)

BAUSCHINGER EFFECT IN THIN METALLIC FILMS BY FEM SIMULATIONS

KIANOOSH MARANDI*, RENAUD VAYRETTE†, THOMAS PARDOEN†, LAURENT DUCHÊNE*, ANNE-MARIE HABRAKEN*

* Department ArGEnCo, Division MS²F,
University of Liège (ULG)
Chemin des Chevreuils 1, 4000 Liège, Belgium
Email: k.marandi@ulg.ac.be, l.duchene@ulg.ac.be, anne.habraken@ulg.ac.be
Web page: http://www.argenco.ulg.ac.be

†Institute of Mechanics, Materials and Civil Engineering, SST/IMMC/IMAP
Université catholique de Louvain (UCL),
Réaumur, Place Sainte Barbe 2, bte L5.02.02 B-1348 Louvain-la-Neuve, Belgium
Email: renaud.vayrette@uclouvain.be, thomas.pardoen@uclouvain.be

Key words: Thin Metallic Films, Bauschinger Effect, Finite Element Simulation, Plastic Deformation.

Abstract. Unpassivated free-standing gold and aluminum thin films (thickness ~ 200-400 nm, mean grain size $d_{m,Au} \approx$ 70-80nm, $d_{m,Al} \approx$ 120-200nm), subjected to tensile tests show Bauschinger effect (BE) during unloading [1, 2]. The focus of this work is to investigate the effect of microstructural heterogeneity such as grain sizes on the BE and the macroscopic deformation behavior in thin metallic films. The finite element code LAGAMINE is used to model the response of films involving sets of grains with different strengths. The numerical results are compared with experimental results from tensile tests on aluminum thin films from the work of Rajagopalan, et al. [2].

1 INTRODUCTION

The ductility of thin metallic films is a key factor in many applications to produce robust devices, including flexible/portable electronics, micro- and nano-electromechanical systems (MEMS/NEMS). Thin films, because of their dimensional and microstructural constraints present a considerably different response compared to bulk size and coarse-grained metals [1, 3]. Unlike coarse-grained polycrystalline metals, where plastic deformation is controlled by dislocations generated from intragranular dislocation sources, in metals with very small grains, other deformation mechanisms such as grain boundary (GB) diffusion and sliding and GB migration, twinning and GB rotation processes compete or cooperate [4, 5].

Reducing the thickness of submicron films often results in strength enhancement but, also, in reduction of the ductility (e.g. [4, 6]). The origin of the strength enhancement in thin films or other nanostructured materials has been widely investigated in both experimental and

modelling areas (e.g. [3, 7-9]). Several models are proposed for the scaling behaviour of flow stress σ_{flow} with the film thickness and grain sizes. This is either formulated by a phenomenological law in the form of $\sigma_{flow} = \sigma_0 + k_1 d^{-n} + k_2 h^{-m}$ where d is the grain size, h is the film thickness, σ_0, k_1, k_2, n and m are positive numerical parameters (e.g.[9-12]), or by more physics-based models that estimate the stress required for the generation/movement of dislocations across slip planes of the film in the general form of $\sigma_{flow} = (1/s)\hat{\mathrm{f}}(s_d, b, h, d, G)$ where s is the Schmid factor, $\hat{\mathrm{f}}$ is a general function of s_d the size of the dislocation source, b the length of the Burgers vector, h the film thickness, d the grain size and G the shear modulus. (e.g. [3, 9, 13, 14]).

Another aspect that influences the deformation behaviour of nanocrystalline metals is the presence of microstructural heterogeneity in the transition regime (defined as the mean grain size of $d_m \approx$ 50-150nm) [2]. Recent investigations on nanocrystalline metals have revealed unusual strain recovery [15] and Bauschinger effect upon unloading of samples subjected to uniaxial tension [1] as a consequence of microstructural heterogeneity. Hence, it is important to consider both microstructural size and heterogeneity in the modeling of mechanical behavior of nanocrystalline materials.

The main objective of this work is to develop FE models to describe the plastic deformation behavior by including the microstructural size and heterogeneity based on experimental stress-strain data and microscopic observations. The J_2 constitutive theory coupled with heterogeneous grain behavior will be employed to examine the correlation between different mechanisms and experimental observations.

2 MICROSTRUCTURAL FEATURES

In the present work, a highly textured aluminum thin film with two major grain orientations, based on experimental results of Rajagopalan, et al [2], is modeled. The Al film is 225 nm thick and was produced by sputter deposition on Si (001) wafer. The Al film exhibited epitaxial growth with only one grain along the thickness and the grains are mainly oriented in two in-plane directions as follows: $\mathrm{Al}(110)||\mathrm{Si}(001)$, $\mathrm{Al}[001]||\mathrm{Si}[110]$ and $\mathrm{Al}(110)||\mathrm{Si}(001)$, $\mathrm{Al}[001]||\mathrm{Si}[1\bar{1}0]$. From the wafer, free-standing Al tensile specimens were fabricated [2].

Figure 1 shows (a) the transmission electron microscopy (TEM), (b) grain size distribution and (c) uniaxial tensile load-unload stress-strain response of the free-standing aluminum film for two loading-unloading cycles. The average grain size is $d_m = 120\ nm$ and the size of the smallest grains is $\approx 0.5 d_m$, and that of the largest is $\approx 2.5 d_m$.

From the in situ TEM deformation observations, there was no dislocation activity observed in the initial linear portions of the stress-strain curves in both cycles (Fig 1(c)). As the strain further increased, dislocation activities started in the relatively larger grains and progressively more grains deformed plastically. This is associated with lower slopes in the stress-strain curves in the loading direction. During unloading, there was no evidence of dislocation activity in the first cycle and film deformed elastically; however at the very end of the second unloading, in which stress has reached larger maximum value during loading than first cycle, dislocation jumps and movement were observed in the larger grains. These dislocation

activities coincide with deviation at the end of the second stress-strain curve and Bauschinger effect.

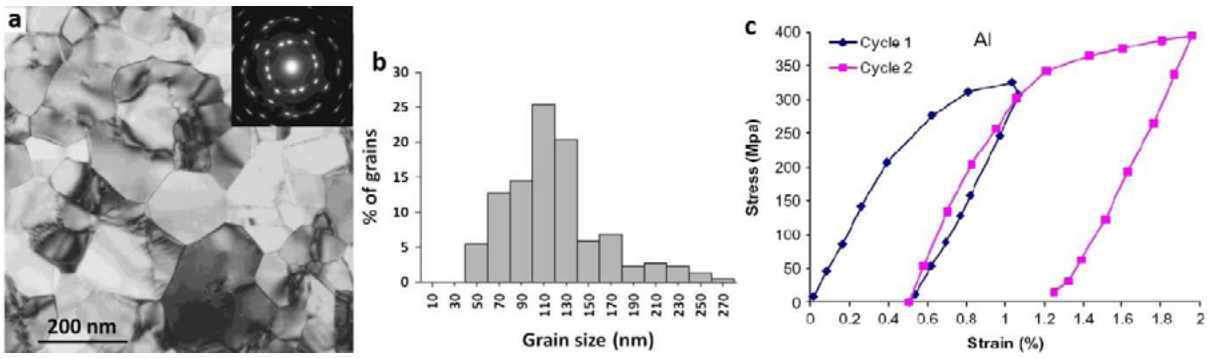

Fig. 1 (a) Bright-field TEM images of aluminum film (thickness=225 nm, d_m=120 nm), (b) histogram of grain size distribution, (c) uniaxial load-unload stress-strain response of free-standing film in tensile test [2].

The source for the observed BE can be explained as, during initial loading, all grains deform elastically and accommodate stresses. With increasing strain, grains that have a greater tendency to plastic deformation, i.e. larger grains and/or grains favourably oriented for plastic deformation, start to deform plastically at low stresses; whereas, smaller grains and/or inauspiciously oriented grains with less tendency to plastic deformation, continue to deform elastically and accommodate stresses at higher levels. This leads to a build-up of internal stresses and a highly inhomogeneous stress distributing in the thin film. During initial stages of unloading, all grains deform elastically, however, upon further unloading the accommodated internal stresses provide the driving force for dislocation activity and plastic deformation in larger grains/favourably oriented grains. This emerges as Bauschinger effect in the stress-strain curve. Such an interpretation of BE was previously presented by Rajagopalan, et al. [2], and confirmed by a simple analytical model.
The aim of the next section is to check whether FE simulations with J_2 plasticity assumption is able to capture BE and whether change in the grain/element patterns affects the overall stress-strain response of the material. This also can assist to understand the importance of the texture and grain sizes on the BE.

3 FINITE ELEMENT SIMULATIONS

The aluminum film, discussed in the previous section, was modelled in the finite element code LAGAMINE. The J_2 theory coupled with heterogeneous grain behavior was employed. The grain size distribution with 12 different sizes (Fig. 1(b)) were more discretized and replaced by three averaged sizes that each is a representative of a group of four grain sizes in ascending order of size.

Table 1 shows the grain size distributions used in the FE simulations.

Table 1: Grain size distributions used in the FE simulations

Grain size	100 nm	150 nm	250 nm
Percentage of grains	56.5%	36%	7.5%

In order to represent the grain size effect on the overall response of the film, two relationships were used to set the flow stress in the grains:

(a) a classical Hall-Petch relationship:

$$\sigma_{flow} = \frac{K_H}{\sqrt{d}} \tag{1}$$

where K_H is a constant and d is the grain size, and

(b) a relationship with the flow stress inversely proportional to the grain size as:

$$\sigma_{flow} = \frac{K_D}{d} \tag{2}$$

where K_D is a constant (e.g., [12]). The second cycle of stress-strain curve in Fig.1(c) is chosen to identify the material parameters of the Al film, and to compare with simulation results. To obtain K_H and K_d, it is assumed that the experimental stress-strain curve corresponds to a film with the average grain size of $d_m = 120nm$, and an overall yielding at 256 MPa (obtained from 0.2% offset strain). This results in

$$K_H = \sigma_{yield}\sqrt{d_m} = 256 \times 10^6 \text{Pa} \times \sqrt{120 \times 10^{-9} \text{m}} = 8.9 \times 10^4\ Pa\sqrt{m} \tag{3}$$

and

$$K_D = \sigma_{yield} d_m = 256 \times 10^6 \text{Pa} \times 120 \times 10^{-9} \text{m} = 30.8\ Pa.m \tag{4}$$

Accordingly, the flow stresses for different grain sizes were estimated using Eqs. (1), (2) and are presented in Table 2:

Table 2: Estimated flow stress for different grain sizes

Grain size	$\sigma_{flow} = K_H/\sqrt{d}$	$\sigma_{flow} = K_d/d$
100 nm	281 MPa	308 MPa
150 nm	230 MPa	205 MPa
250 nm	178 MPa	123 MPa

Figure 2(a) and Fig. 2(b) show the estimated stress-strain responses for the grain sizes of the Table 2 along with the experimental data for the Al film. In the estimations, it has been assumed that the work hardening rates of the grains with different sizes are similar to that of the experimental data.

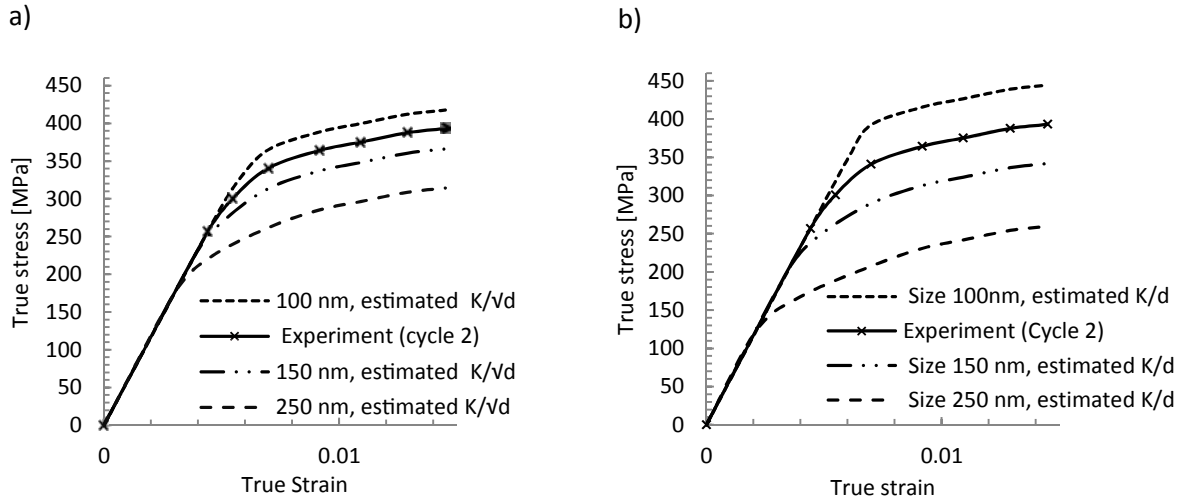

Fig. 2 Estimated stress-strain responses for different grain sizes assuming that the flow stress obeys (a) a Hall-Petch equation, (b) a relationship with an inverse proportionality to the grain sizes.

It can be seen that the estimated stress-stain curves obtained by using Eq. (1) are less scattered than curves estimated by using of Eq. (2) for the flow stresses.
The two sets of estimated grain responses (Fig. 2(a), 2(b)) were individually input to the finite element code to simulate two Al films with different degrees of microstructure heterogeneity. Assuming that J_2 plasticity and isotropic hardening behaviour are prevailed, the stress-strain responses of the films comprising three constituent phases were simulated. The FE simulations used 20×10×1 three-dimensional continuum-brick elements to model cyclic tensile tests of the samples with the dimensions of 1000 nm×500 nm×50 nm. The FE model consists of three different grain sizes, i.e. 100 nm, 150 nm and 250 nm, used to simulate the tensile tests is shown in Fig. 3.

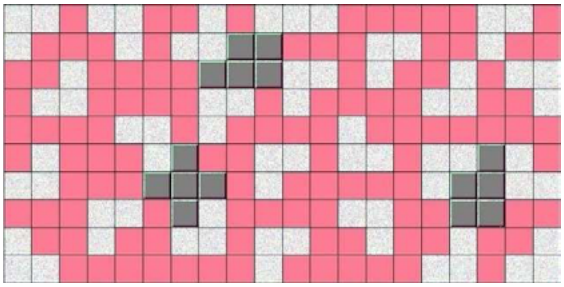

Fig. 3 Finite element model with pattern of the grains.

The stress-strain simulation results and experimental data for the tensile tests on the heterogeneous FE models comprising three constituent phases by presuming the Hall-Petch strengthening and that with strength inversely proportional to the grain sizes are presented in Fig. 4 and Fig. 5, respectively.

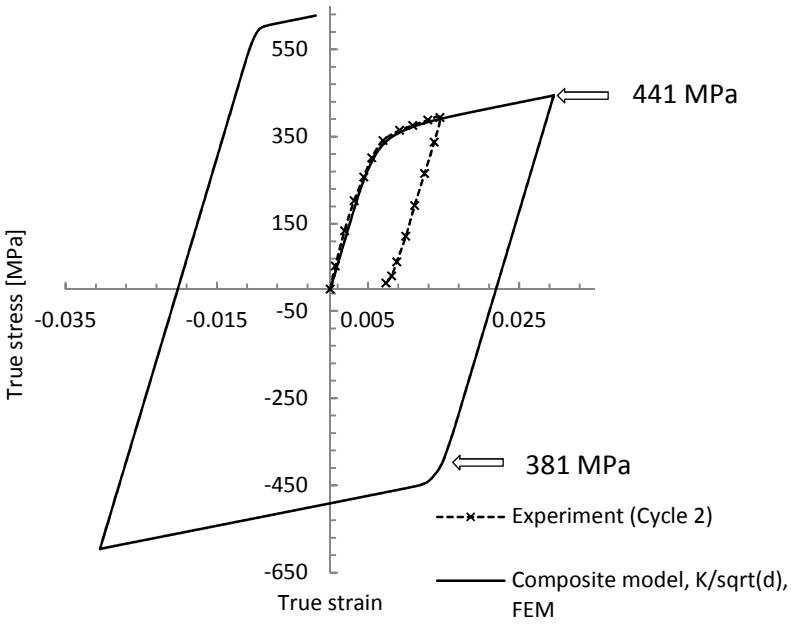

Fig. 4 Comparison of tensile stress-strain responses for the FE composite model with the assumption of $\sigma_{flow}=K_H/\sqrt{d}$ and experimental data.

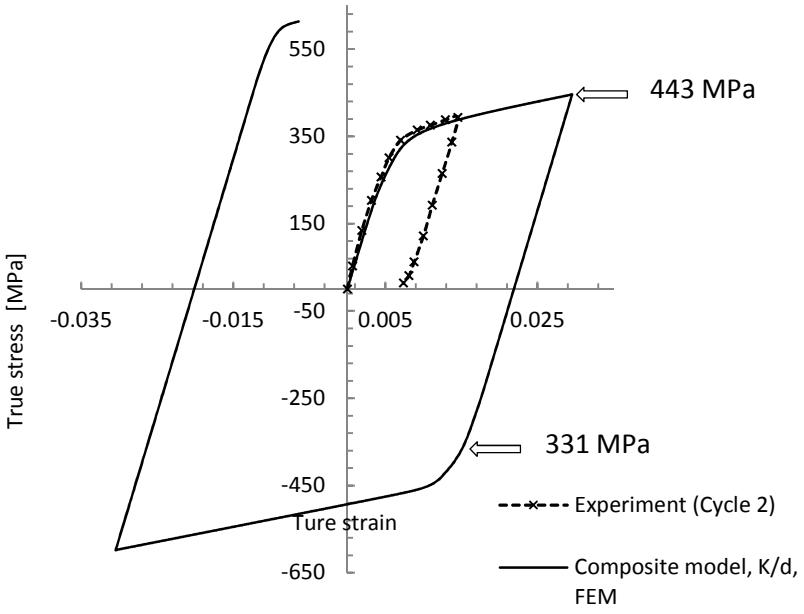

Fig. 5 Comparison of tensile stress-strain responses for the FE composite model with the assumption of $\sigma_{flow}=K_d/d$ and experimental data.

It can be seen that, for both simulations, the stress-strain curves correlate well with the experimental responses in the forward loading direction and there are some degrees of

Bauschinger effect in the simulated stress-strain curves. The BE is recognized as deviation from the linear stress-strain response in the reverse loading direction at a lower absolute stress value than the ultimate stress in the forward loading direction; noting that the FE simulations use an isotropic hardening von Mises plasticity material formulation. By comparing Fig. 4 and Fig. 5, it is concluded that the FE model with more heterogeneous material properties results in the larger degree of BE. However, the magnitude of the BE in both simulations are far less than the BE observed in the experimental data. It should be mentioned that FE simulations were achieved up to a larger strain than the experimental data for having more distinct Bauschinger effects.

To examine whether the distribution pattern of the constituent phases affects the overall simulation stress-strain responses, each of the phases were randomly distributed among the elements, while the volume fraction of each phase was kept fixed to be the same as the prior simulations (Fig. 6).

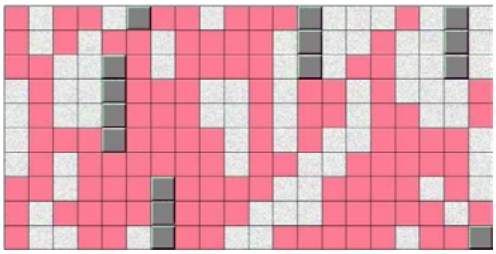

Fig. 6 Random distribution pattern of the elements

It was observed that there was no significant change in the overall stress-strain responses between the simulations using the random pattern of Fig. 6 and the granulated pattern of Fig. 3 with identical material properties of the constituent phases for both simulations (results are not illustrated here), and therefore, the effect of element patterns were negligible.

CONCLUSIONS

The simulations show that BE are, among other possible sources, the result of inhomogeneous stress distribution caused by microstructural heterogeneity. It is also observed that use of an isotropic hardening von Mises plasticity material and a Hall-Petch relationship and/or a relationship with inverse proportionality to the grain sizes for the flow stresses are not sufficient to produce a large degree of the BE as much as seen in the experimental data. Future works could include:

- Investigating the effect of grain orientations on the flow stress. This could be examined by employing a crystal plasticity model instead of the J_2 plasticity. The grain orientations is believed to have large impact on the BE [2].
- Employing more comprehensive models such as the Source Model [9] where the flow stress is a function of the film thickness, the size of the dislocation sources and the grain orientations.

ACKNOWLEDGEMENTS

This research has been funded by the Interuniversity Attraction Poles Programme initiated

by the Belgian Science Policy Office, IAP7/21.

REFERENCES

[1] Rajagopalan, J., J.H. Han, and M.T.A. Saif, *Bauschinger effect in unpassivated freestanding nanoscale metal films.* Scripta Materialia, 2008. **59**(7): p. 734-737.
[2] Rajagopalan, J., et al., *In situ TEM study of microplasticity and Bauschinger effect in nanocrystalline metals.* Acta Materialia, 2010. **58**(14): p. 4772-4782.
[3] Arzt, E., *Size effects in materials due to microstructural and dimensional constraints: a comparative review.* Acta Materialia, 1998. **46**(16): p. 5611-56265626.
[4] Mompiou, F., et al., *Inter- and intragranular plasticity mechanisms in ultrafine-grained Al thin films: An in situ TEM study.* Acta Materialia, 2013. **61**(1): p. 205-216.
[5] Chen, M., et al., *Deformation twinning in nanocrystalline aluminum.* Science, 2003. **300**(5623): p. 1275-1277.
[6] Coulombier, M., et al., *Imperfection-sensitive ductility of aluminium thin films.* Scripta Materialia, 2010. **62**(10): p. 742-745.
[7] Fleck, N.A., et al., *Strain gradient plasticity: theory and experiment.* Acta Metallurgica et Materialia, 1994. **42**(2): p. 475-487487.
[8] Nicola, L., E. Van Der Giessen, and A. Needleman, *Two hardening mechanisms in single crystal thin films studied by discrete dislocation plasticity.* Philosophical Magazine, 2005. **85**(14): p. 1507-1518.
[9] Gruber, P.A., et al., *Size effects on yield strength and strain hardening for ultra-thin Cu films with and without passivation: A study by synchrotron and bulge test techniques.* Acta Materialia, 2008. **56**(10): p. 2318-2335.
[10] Venkatraman, R. and J.C. Bravman, *Separation of film thickness and grain boundary strengthening effects in Al thin films on Si.* Journal of Materials Research, 1992. **7**(8): p. 2040-2048.
[11] de Boer, M.P., et al., *On-chip laboratory suite for testing of free-standing metal film mechanical properties, Part II – Experiments.* Acta Materialia, 2008. **56**(14): p. 3313-3326.
[12] Nix, W.D., *Mechanical properties of thin films.* Metallurgical Transactions A, 1989. **20**(11): p. 2217-2245.
[13] Von Blanckenhagen, B., P. Gumbsch, and E. Arzt, *Dislocation sources in discrete dislocation simulations of thin-film plasticity and the Hall-Petch relation.* Modelling and Simulation in Materials Science and Engineering, 2001. **9**(3): p. 157-169.
[14] Yoonjoon, C. and S. Suresh, *Size effects on the mechanical properties of thin polycrystalline metal films on substrates.* Acta Materialia, 2002. **50**(7): p. 1881-18931893.
[15] Rajagopalan, J., J.H. Han, and M.T.A. Saif, *Plastic deformation recovery in freestanding nanocrystalline aluminum and gold thin films.* Science, 2007. **315**(5820): p. 1831-1834.